DATE ISSUED MAY 29 1981

800828

ORNL/TM-7533

ORNL
MASTER COPY

ornl

OAK
RIDGE
NATIONAL
LABORATORY

UNION
CARBIDE

Coal Conversion Solid Wastes: Characterization for Environmental Assessment

S. Y. Lee
W. J. Boegly, Jr.

ENVIRONMENTAL SCIENCES DIVISION
Publication No. 1692

OPERATED BY
UNION CARBIDE CORPORATION
FOR THE UNITED STATES
DEPARTMENT OF ENERGY

Printed in the United States of America. Available from
National Technical Information Service
U.S. Department of Commerce
5285 Port Royal Road, Springfield, Virginia 22161
NTIS price codes—Printed Copy: A04 Microfiche A01

This report was prepared as an account of work sponsored by an agency of the United States Government. Neither the United States Government nor any agency thereof, nor any of their employees, makes any warranty, express or implied, or assumes any legal liability or responsibility for the accuracy, completeness, or usefulness of any information, apparatus, product, or process disclosed, or represents that its use would not infringe privately owned rights. Reference herein to any specific commercial product, process, or service by trade name, trademark, manufacturer, or otherwise, does not necessarily constitute or imply its endorsement, recommendation, or favoring by the United States Government or any agency thereof. The views and opinions of authors expressed herein do not necessarily state or reflect those of the United States Government or any agency thereof.

ORNL/TM-7533

Contract No. W-7405-eng-26

COAL CONVERSION SOLID WASTES: CHARACTERIZATION FOR ENVIRONMENTAL ASSESSMENT

42 42

S. Y. Lee and W. J. Boegly, Jr.

42

ENVIRONMENTAL SCIENCES DIVISION

Publication No. 1692

Date Published: June 1981

NOTICE This document contains information of a preliminary nature. It is subject to revision or correction and therefore does not represent a final report.

OAK RIDGE NATIONAL LABORATORY
Oak Ridge, Tennessee 37830
operated by
UNION CARBIDE CORPORATION
for the
DEPARTMENT OF ENERGY

ACKNOWLEDGMENTS

The authors wish to acknowledge the following personnel for their contributions to this report. H. W. Wilson and S. K. Hall provided technical support. G. T. Yeh developed the dissolution model used in this study. We thank E. Davis, R. R. Turner, C. W. Francis, and T. Tamura for reading the manuscript and offering helpful suggestions.

ABSTRACT

LEE, S. Y., and W. J. BOEGLY, Jr. 1981. Coal conversion solid wastes: Characterization for environmental assessment. ORNL/TM-7533. Oak Ridge National Laboratory, Oak Ridge, Tennessee. 46 pp.

Physicochemical and leaching properties of coal conversion solid wastes produced by British Gas-Lurgi, Cogas, and Texaco gasification pilot plants were measured in order to assess the potential environmental impact caused by disposal of these wastes. The British Gas-Lurgi waste was composed of homogeneous calcic aluminosilicate glass with less than 1% of metallic iron particles. Major and trace elements were diluted by the influx of limestone added during the slagging process. The Cogas waste was partially vitrified ferruginous aluminosilicate with a surface occasionally covered by iron oxide coatings. Immiscible iron oxide and iron sulfide phases in the aluminosilicate matrix of ferromagnetic particles were detected. The Texaco gasification waste was composed of sulfur-rich ferruginous aluminosilicate particles, and the surface of the particles was extensively coated by amorphous iron sulfide and occasionally by lepidocrocite. Pyrrhotite mineral was dominant in the ferromagnetic fraction. In spite of wide variations in heavy metal content of the bulk wastes, some of the chalcophile-group elements displayed consistent association in the surface coatings and ferromagnetic fraction of the wastes. The trace element concentrations (Cd, Cr, Pb, As, Hg, Se, Ag) in the solid waste leachates obtained by the proposed ASTM method were below the limits established by the Interim Primary

Drinking Water Standard. In equilibrium batch-leaching studies, the first-order dissolution rates of Ca, Al, Fe, Ni, and SO_4 from the solid wastes were found to be very slow ($k < 0.17/d$).

TABLE OF CONTENTS

	Page
ABSTRACT	v
LIST OF TABLES	ix
LIST OF FIGURES	xi
INTRODUCTION	1
EXPERIMENTAL	2
Materials	2
Methods	4
RESULTS	7
Physical Properties	7
Chemical and Mineralogical Properties	13
Leaching Properties	18
DISCUSSION	28
REFERENCES	33

LIST OF TABLES

Table		Page
1	Physical properties of coal conversion solid wastes from the three processes studied	8
2	Chemical composition of unfractionated and ferromagnetic fraction of British Gas-Lurgi, Cogas, and Texaco solid wastes	14
3	Batch leaching results of British Gas-Lurgi, Cogas, and Texaco solid wastes obtained by proposed American Society for Testing and Materials Methods	19
4	Concentrations of selected elements in leachates of British Gas-Lurgi, Cogas, and Texaco solid wastes	21
5	Estimated dissolution constants obtained from equilibrium batch leaching experiments of British Gas-Lurgi, Cogas, and Texaco solid wastes	23

LIST OF FIGURES

Figure		Page
1	Scanning electron micrographs and x-ray spectra of British Gas-Lurgi solid waste	9
2	Scanning electron micrographs and x-ray spectra of Cogas solid waste	11
3	Scanning electron micrographs and x-ray spectra of Texaco solid waste	12
4	X-ray diffractograms of ground ferromagnetic fractions from solid wastes	16
5	"Best fit" dissolution curve and equations for the British Gas-Lurgi and Cogas wastes	26
6	"Best fit" dissolution curve and equations for the Texaco waste	27
7	Range of selected trace element concentrations in combustion solid wastes (fly and bottom ashes) and conversion solid wastes including the British Gas-Lurgi, Cogas, and Texaco	30

INTRODUCTION

Coal conversion technology is being developed to utilize relatively abundant coal resources for the production of synthetic gas and liquid fuels. Evaluations of technical and economical viability of near-commercial-scale coal conversion demonstration plants are in progress (Jones et al., 1978). Since coal conversion plants will consume vast amounts of coal and produce voluminous solid wastes, an evaluation of the environmental acceptability of each conversion process has been undertaken prior to full-scale commercialization (Boegly, 1978).

Disposal of solid wastes from coal conversion facilities could be a potential problem because the hazardous contaminants leached from the wastes could have a profound effect on water quality of the region (Morris et al., 1979). Existing laws may adequately regulate the release of gaseous and aqueous effluents to the environment, but the complex nature of solid wastes makes it difficult to establish clear and effective regulations for their disposal. The U.S. Congress passed the Resource Conservation and Recovery Act (RCRA), which provides for federal regulation of the treatment and disposal of solid wastes that represent a potential danger to the environment or to human health.

To implement the RCRA, the Environmental Protection Agency (EPA) issued a regulation concerning the identification and disposal of hazardous waste. The regulation requires a leaching test (extraction procedure) to evaluate toxicity characteristics of wastes. Leachability of solid wastes depends on the chemical form of its

components, the physical properties of the solid, and the composition of the aqueous leaching medium. The results of leaching tests will also depend on the experimental conditions such as the solid-to-solution ratio and equilibrium time for batch leaching and the application method and residence time of the leaching solution for column leaching. The various experimental methods used for leaching tests lead to difficulties in comparing data obtained in one set of leaching experiments with another set (Hespe, 1971). Establishment of a standard leaching method for solid waste is, therefore, highly desired. Such a standard method should be practical as well as useful for the accurate prediction of the long-term leaching behavior of solid wastes which have been disposed of in the environment.

The objectives of this study were to characterize the physicochemical properties and to evaluate the leaching behavior of solid wastes produced by three coal conversion pilot plants. The research was intended to provide pertinent information for environmental assessment of the DOE/FE proposed demonstration plants and for the development of a disposal technology for coal conversion solid wastes.

EXPERIMENTAL

Materials

Relatively large quantities (0.3×10^4 to 1×10^4 kg) of solid wastes were obtained from the British Gas-Lurgi, Cogas, and Texaco gasification pilot plants. The British Gas-Lurgi solid waste was produced by British Gas Co., Westfield, Scotland. The process used a

fixed-bed countercurrent oxygen-blown gasifier to convert high-sulfur bituminous coal (Pittsburgh No. 8) into gaseous products. The coal ash formed in the combustion zone melted and mixed with limestone flux to make a free-flowing solid solution (slag). The slag that formed in the bottom of the gasifier flowed through a tap hole into a water-quenching vessel.

The Cogas waste was received from the pilot plant operated by the British Coal Utilization Research Association at Leatherhead, England. The process employed a coupled system of pyrolysis and gasification to convert coal (Illinois No. 5 and 6) into natural gas and fuel oil. Char from the pyrolysis section was fed to the gasifier where it was converted to gas with heated steam and air. The slagging combustor (fluidized bed) consumed most of the carbon remaining in the ash and produced the hot flue gas as a heat source. The solid waste from the combustor was water-quenched.

The gasified SRC-II vacuum bottoms were received from the Texaco gasification pilot plant at Montebello, California. The SRC-II process included liquefaction, fractionation, vacuum separation, and gasification stages. The pulverized coal (Kentucky No. 9/14) was mixed with a solvent and hydrogen and sent to a dissolver, in which most of the organic materials were liquefied. The liquefied slurry passed through vapor-liquid separators and fractionators. When the slurry residues of the process reached the vacuum tower, the organic phase remaining in the slurry was separated from the inorganic residue. The waste received from the Montebello gasification pilot plant was the gasified bottom ash (entrained bed) of the residue (vacuum bottoms) produced by the SRC-II liquefaction pilot plant at Ft. Lewis, Washington.

Methods

About 10 kg of the solid wastes were air-dried and stored for characterization and leaching experiments. Physical properties such as bulk density, particle density, and particle size distribution were determined by standard analytical methods. In addition, approximately 50 g of each sample was heated in a muffle furnace for 5 h to determine ignition losses at selected temperatures.

Morphology of the waste particles was examined by a scanning electron microscope (SEM). Ferromagnetic particles were separated from about 200 g of the samples by a horseshoe magnet. A small portion (about 80 mg) of magnetic and nonmagnetic fractions was embedded in epoxy resin by using a metallographic specimen molder (3 cm in diameter). The resin block was polished until the cross section of the embedded particles was exposed. Qualitative chemical composition of solid phases on the polished surface was determined using an energy dispersive x-ray analyzer (EDX) attached to the SEM.

About 10 g of the bulk samples and 5 g of the magnetic fractions were ground with an agate mortar until the ground samples passed through a 150-mesh (106 μm in diameter) sieve. A portion of the ground samples was used for x-ray diffraction analysis, and the remainder was used for elemental analysis. Inductive coupled argon plasma atomic emission spectroscopy (EPA, 1977) was used to determine the concentration of most elements after HNO_3-HCl-HF digestion of the ground samples. Total sulfur and carbon contents were determined, respectively, using an automatic LECO titrator and a carbon combustion

train analyzer. Arsenic concentration in the leachates was determined by an improved helium glow detector method (Feldman, 1979), and Hg concentration was determined by the stannous chloride reduction technique (ORNL, 1979a). Other elements in leachates were determined by atomic absorption spectroscopy.

Laboratory leaching experiments were performed in two ways: the proposed ASTM method (Leaching of Waste Materials, 1978, published as information by ASTM) and a batch equilibrium method. The proposed ASTM method included sodium acetate-acetic acid buffer (method B) and water (method A) extractions. The solution for the sodium acetate (NaOAc) method was prepared by dissolving 3.7 g of sodium acetate and 4.9 g of glacial acetic acid (HOAc) in 1000 ml of deionized water and adjusting the pH of the solution to 4.5 by adding an HOAc or NaOH solution. Deionized water was used for the water extraction. Two-hundred-gram aliquots of each solid waste were equilibrated with 800 ml of each extraction solution in 1000-ml plastic bottles. The bottles were shaken for 48 h on a reciprocating platform shaker. The leachates were filtered through 0.45-μm membrane filters (cellulose acetate) and then analyzed for the selected trace elements.

For the batch equilibrium method, 600 g of solid wastes were equilibrated in 6 liters of deionized water in 8-liter plastic bottles, and the bottles were shaken manually twice a week. After a designated equilibration time period, the bottle was shaken for 2 min, and an aliquot (25 ml) of leachate was taken. The influence of removal of the small aliquots from the large batch was assumed insignificant on the overall rate of dissolution. The aliquots of leachate were filtered

through 0.45-μm membrane filters and then analyzed. The differential equations governing the batch equilibrium leaching conditions were derived from the conservation of mass laws, which assumed that the dissolution system would reach the equilibrium state linearly (first-order rate) and the dissolution would be limited by the solubility of the components (Yeh, 1980):

$$V \frac{\partial C_w}{\partial t} = - W \frac{\partial C_s}{\partial t} \quad , \tag{1}$$

$$\frac{\partial C_s}{\partial t} = - \frac{k}{R_d} (C_s - D_d C_w) \quad , \tag{2}$$

where V = volume of water (ml), C_w = concentration of dissolved element in the solution (μg/ml), W = weight of waste (g), C_s = concentration of an element in the waste (μg/g), k = dissolution rate constant, $R_d = (1 + D_d W V^{-1})$ which is the retardation coefficient at equilibrium, D_d = dissolution distribution coefficient (C_s/C_w) at equilibrium, t = time (day). The solution of Eqs. (1) and (2) subject to C_w was

$$C_w = C_f (1 - e^{-kt}) + C_i \quad , \tag{3}$$

where $C_f = (C_s^o W V^{-1} R_d^{-1}) + C_i (R_d^{-1} - 1)$, which represents the functional concentration (μg/ml) of an element dissolved from solids as a function of rate and time (t) in the manner of apparent first order kinetic reaction. C_s^o = initial concentration of an element in the waste (μg/g); C_i = estimated concentration (μg/ml) of an element released readily from solid over a small finite time period.

The constants k, C_i and R_d were estimated from Eq. (3) using a nonlinear least-square regression analysis in which time (t) and element concentration in solution (C_w) were dependent and independent variables, respectively.

RESULTS

Physical Properties

The coal conversion solid wastes studied were composed of irregular gray or black particles with wide ranges of particle sizes (Table 1). The particle size of British Gas-Lurgi waste was dominated by 0.5- to 2-mm sizes. Cogas waste had a large mean particle size, and about 87% of the waste by weight belonged to the particle sizes between 2 and 9.5 mm. The dominant particle sizes of Texaco waste were 0.05- to 2-mm sizes, and aggregates of fine particles were commonly observed in the waste. The dehydration of minerals as well as volatilization of some elements in the waste contributed to the ignition losses of the waste. The particle densities of the wastes (Table 1) were in the ranges of common silicate minerals (2.5 - 2.8 g cm^{-3}). The waste with the largest mean particle size has the lowest bulk density (Table 1), which would require more landfill volume for a unit weight of waste.

British Gas-Lurgi waste was composed of varying sizes of sharp-edged platy and blocky particles (Fig. 1A). The voids formed by inclusion of gas phases in the solid solution were rarely depicted on the surface of the cross section of nonmagnetic calcium silicate

Table 1. Physical properties of coal conversion solid wastes from the three processes studied

Property	Processes		
	British Gas-Lurgi	Cogas	Texaco
Color	Charcoal gray	Brownish black	Brownish gray
Shape of particle	Platy & blocky	Blocky	Granular
Mean particle size, mm[a]	1.05 ± 0.53	4.30 ± 2.46	0.55 ± 0.12
Bulk density, g/cm^3	1.47	1.37	1.72
Particle density, g/cm^3	2.76	2.66	2.58
Ignition loss, %			
at 100°C	1.72	2.20	0.62
at 500°C	0	0.06	2.19
at 800°C	-1.20[b]	0.14	2.51
Magnetic fraction, %	1	5	7

[a]Geometric mean particle size ± one standard deviation.

[b]Negative means weight gain.

ORNL-PHOTO Y169239

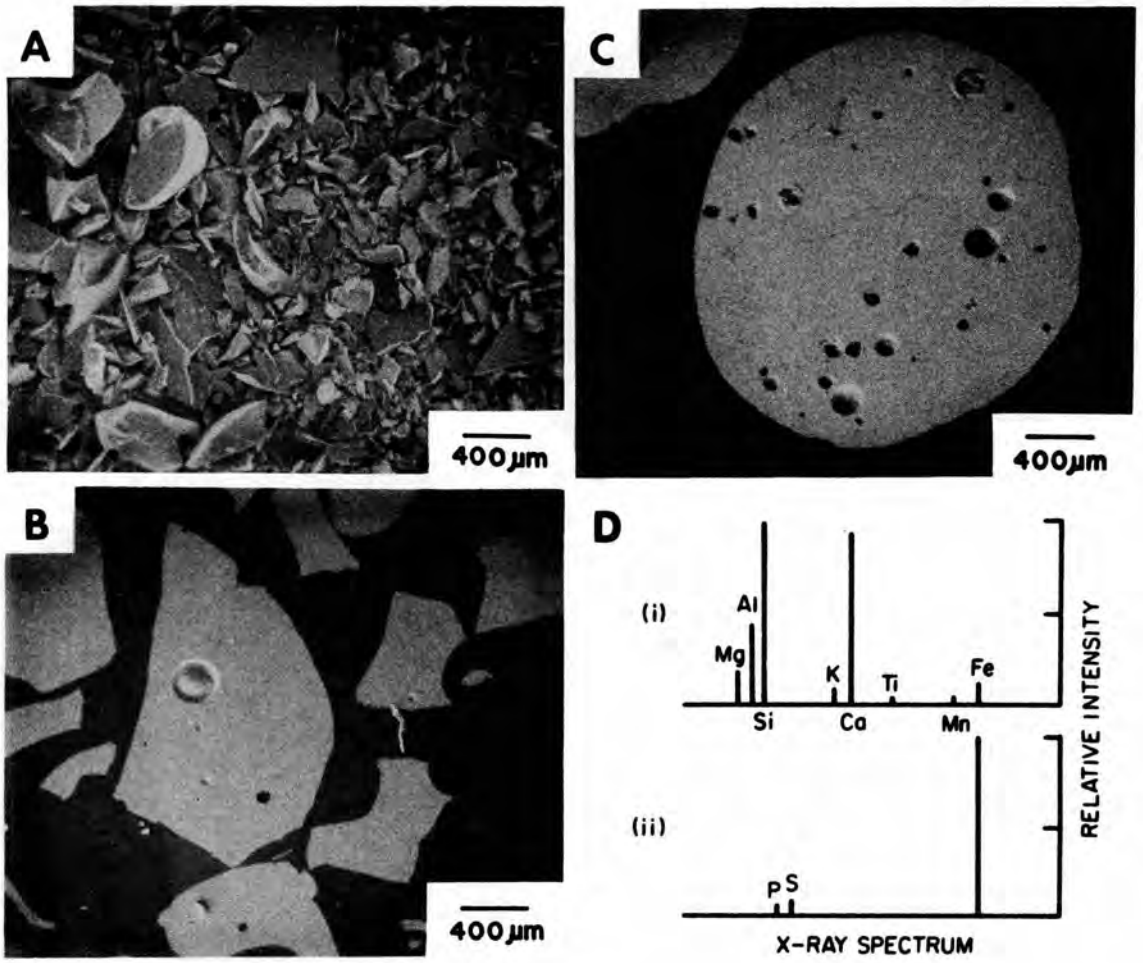

Fig. 1. Scanning electron micrographs and x-ray spectra of British Gas-Lurgi solid waste. (A) General view of the waste particles; (B) cross section of nonmagnetic fraction of the waste; (C) cross section of magnetic fraction; (D) x-ray spectrum of (i) nonmagnetic particle and (ii) magnetic particle.

particles (Fig. 1B). On the other hand, the gas voids were common on the cross section of spherical ferromagnetic particles (Fig. 1C). The ferromagnetic particles were about 1% of the waste by weight and 1 to 5 mm in diameter.

The morphology of Cogas waste was more complex than that of British Gas-Lurgi waste. Relatively large and angular blocky particles were dominant in the Cogas waste; however, smaller quantities of spherical, porous, and elongate particles were also depicted (Fig. 2A). Some of the small blocky and porous particles and most of the spherical particles were ferromagnetic. The ferromagnetic fraction comprised about 5% of the total weight. The relatively large blocky particles had fairly clean surfaces, but the surfaces of the spherical and porous particles were covered with powdery and crusty coatings. Varying sizes of voids were common on the surface of the cross section of the spherical particles but were not common on the surface of the blocky particles (Fig. 2C).

In Texaco waste, varying sizes of spherical particles and aggregates of small spherical particles were the major components (Fig. 3A). Angular blocky glass particles were one of the major components of coarser particles. Fine powdery particles (< 0.053 mm) and aggregates of the fine particles were common in the sample. The spherical particle surfaces were covered extensively by powdery or crusty coatings. About 7% of the total weight was composed of a magnetic fraction, of which the surface was less extensively coated with the crusty coatings as compared with the nonmagnetic particles. Blister-shaped coatings and voids were observed on the cross section of the nonmagnetic particles (Fig. 3B and D).

ORNL-PHOTO Y169240

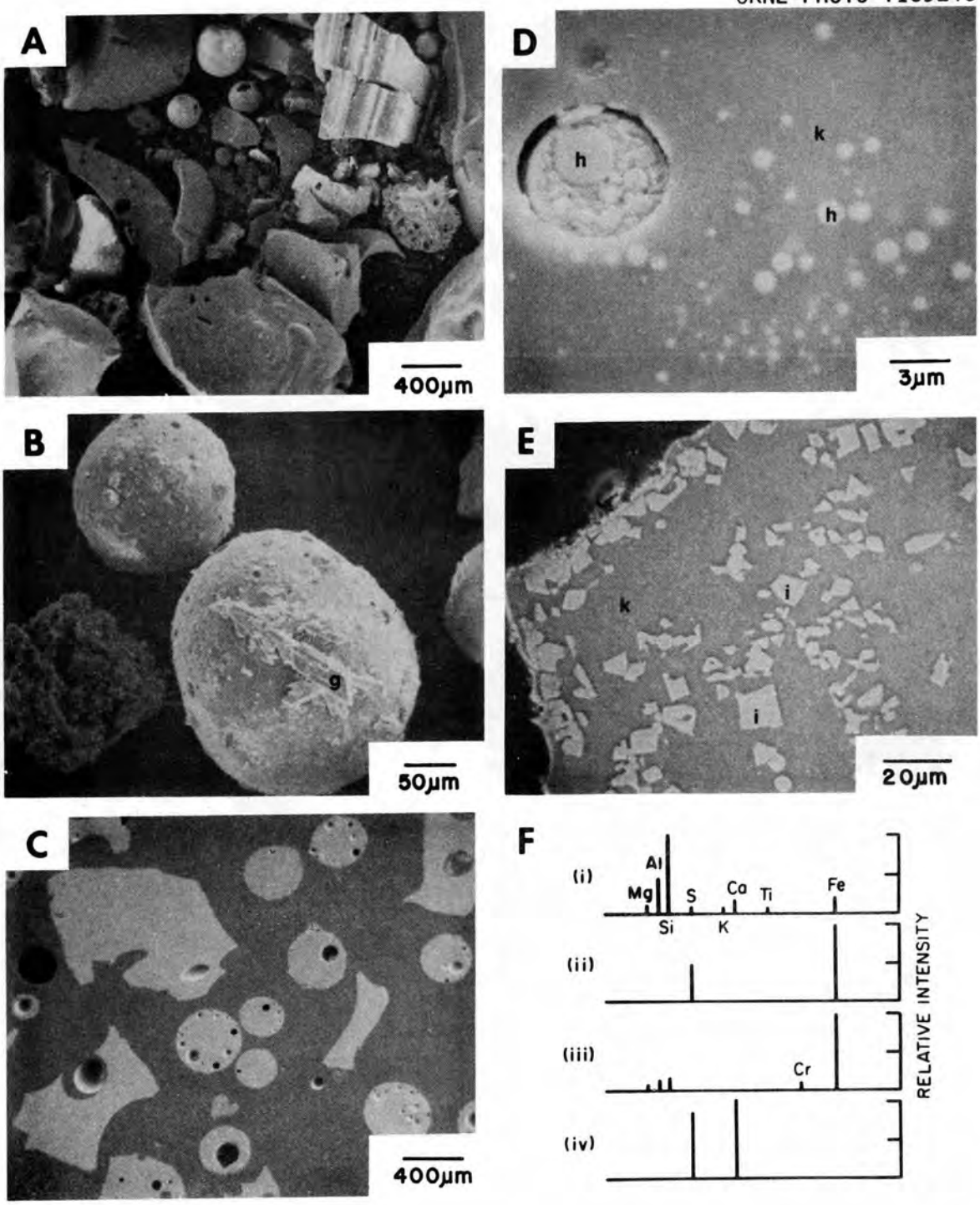

Fig. 2. Scanning electron micrographs and x-ray spectra of Cogas solid waste. (A) General view of waste particles; (B) closeup of magnetic particles and gypsum crystal (g) on the surface of a spherical particle; (C) cross section of magnetic particles; (D) closeup view of iron sulfide inclusion (h) in a spherical magnetic particle; (E) closeup view of iron oxide (i) in an angular magnetic particle; (F) x-ray spectrum of matrix (i) of magnetic (area k in D and E) and nonmagnetic particles, (ii) iron sulfide inclusion (h in D), (iii) iron oxide (i in E), and (iv) gypsum (g in B).

ORNL-PHOTO Y169241

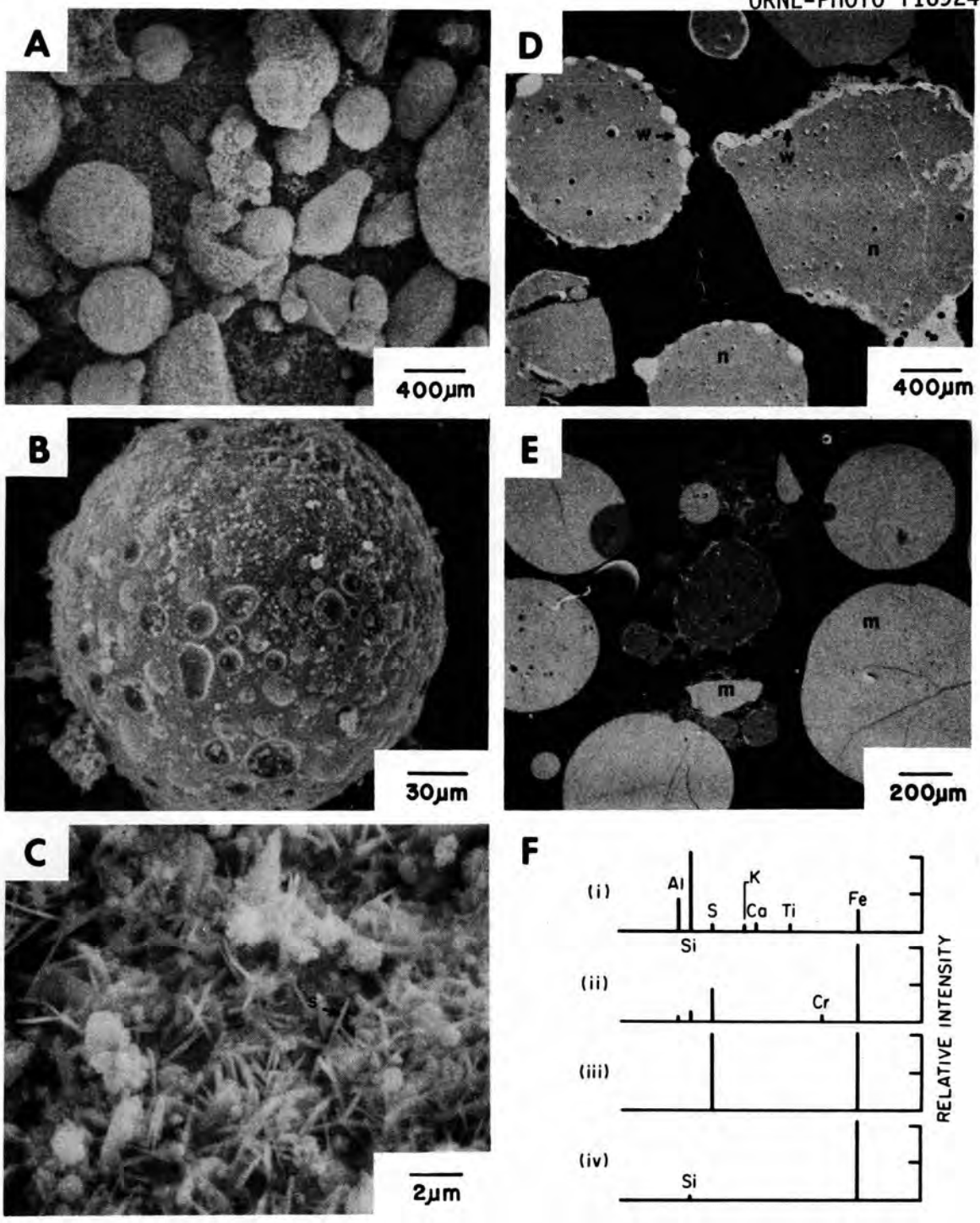

Fig. 3. Scanning electron micrographs and x-ray spectra of Texaco solid waste. (A) General view of waste particles; (B) close-up view of a nonmagnetic particle; (C) iron hydroxide particles on the surface of a ferromagnetic particle (arrow s); (D) cross section of nonmagnetic particles with extensive iron sulfide coating (arrow w); (E) cross section of ferromagnetic particles (area m) with nonmagnetic particles and aluminosilicate phase (area n); (F) x-ray spectrum of (i) aluminosilicate phase (area n in D and E), (ii) coatings on the surface of nonmagnetic particles (arrow w in D), (iii) matrix of ferromagnetic particles (area m in E), and (iv) rod-shaped particles (arrow s in C).

Chemical and Mineralogical Properties

Major and trace elemental compositions of the unfractionated whole wastes and the ferromagnetic fraction of the wastes are presented in Table 2. The chemical analyses revealed that British Gas-Lurgi waste was composed of calcic aluminosilicate. The amounts of Ca and Mg among major elements and Mn among trace elements in the British Gas-Lurgi sample were significantly higher than in the other wastes. The source of these enriched elements (Ca, Mg, and Mn) in British Gas-Lurgi waste was the limestone flux added during the slagging process. The added limestone flux diluted the concentration of selected trace elements (Ni, Cr, Mo, Co, Cu, and B) in the ash, which were contributed by the feed coal. The magnetic fraction of British Gas-Lurgi waste was composed largely of iron with trace amounts of S and P (Fig. 1D). The chemical analyses suggested that the magnetic particles were the metallic form of iron rather than the oxide form (Table 2). The intensity ratios of x-ray spectra (EDX) of major elements (Fig. 1D) in the different areas of nonmagnetic particles varied less than 5%, and no apparent phase boundaries on the cross-section surface of the particles were observed under the high magnifications of backscattering and normal scanning mode of SEM. The XRD analysis did not reveal detectable amounts of crystalline minerals in the waste. These results indicated that the British Gas-Lurgi waste is a chemically homogeneous glass mixed with a very small amount of metallic iron particles.

Cogas waste had larger amounts of Si, Fe, and Al, and lesser amounts of Ca and Mg in comparison with British Gas-Lurgi waste

Table 2. Chemical composition of unfractioned and ferromagnetic fraction of British Gas-Lurgi, Cogas, and Texaco solid wastes

Element	British Gas-Lurgi		Cogas		Texaco	
	Unfractionated	Magnetic fraction	Unfractionated	Magnetic fraction	Unfractionated	Magnetic fraction
			Major elements (%)			
Al	8.8	0.4	10.1	10.2	8.8	6.3
Ca	18.5	0.8	2.9	2.7	2.2	1.4
Fe	3.8	89.6	13.4	14.1	17.2	34.1
K	0.6	<0.1	1.5	1.3	1.4	0.9
Mg	4.9	0.2	0.8	0.7	0.5	0.3
Na	0.3	<0.1	1.8	1.6	0.2	0.1
Ti	0.5	<0.1	0.6	0.5	0.6	0.4
Si	17.9	a	22.5	20.4	20.1	13.7
S	0.4	a	0.3	0.8	3.8	11.8
C	1.0	a	1.8	a	1.7	a
			Trace elements (μg/g)			
Ag	1.0	a	0.3	0.4	0.3	0.9
B	287.3	35.2	1302.2	1153.0	590.7	335.0
Ba	654.5	35.0	454.0	427.0	531.0	219.0
Be	10.3	0.1	18.1	20.3	12.6	8.5
Cd	1.0	91.2	0.8	a	1.6	a
Ce	146.5	0.7	85.2	93.8	25.9	53.4
Co	7.2	764.7	137.3	139.9	33.7	117.0
Cr	78.1	93.1	386.1	360.0	642.6	435.0
Cu	29.8	1031.8	61.9	120.0	93.5	322.0
Li	86.3	6.6	80.7	69.1	63.7	37.6
Mn	3987.2	369.4	425.4	450.0	293.2	228.0
Mo	4.0	263.4	18.8	37.6	72.6	273.0
Nb	17.2	a	11.9	16.7	1.7	a
Ni	73.0	2515.7	254.0	348.0	150.0	488.0
P	466.7	9183.2	275.5	333.0	436.3	359.9
Sc	30.2	a	24.4	20.4	19.3	13.3
Sr	519.8	24.5	503.3	448.0	182.1	120.0
Th	28.8	0.9	16.2	19.8	15.8	15.1
V	154.3	60.9	237.2	220.0	449.5	408.0
Y	54.8	3.9	53.6	46.1	41.1	30.9
Zn	8.3	101.2	65.7	103.0	96.1	97.3
Zr	191.7	a	196.6	173.0	170.2	105.0

[a]Not determined.

(Table 2). The trace elements frequently associated with coal ash were also higher in the Cogas waste. Small differences in chemical composition between the unfractionated sample and magnetic fraction were noticed. Compared to the unfractioned sample, the magnetic fraction was slightly enriched in Fe and S, and moderately enriched in Ni, Zn, Mo, and Cu. The apparent association of the trace elements with Fe and S suggests that the trace elements are in the feed coal as impurities of iron or sulfide minerals and that they remain with the iron- and sulfide-bearing components in the wastes.

Qualitative analysis based on the intensity ratios of elements by x-ray spectroscopy indicated that major elements making up aluminosilicate glass in the Cogas waste were uniformly distributed (Fig. 2F-i). In the cross section of spherical magnetic particles, varying sizes of spherical solid inclusions were observed (Fig. 2D). The inclusions were composed of Fe and S with an x-ray intensity ratio of 2 to 1 (Fig. 2F-ii). The irregularly shaped inclusions in the cross section of blocky magnetic particles (marked i in Fig. 2E) were iron oxides with small amounts of Cr impurity (F-iii). A trace amount of Ni was detectable by X-ray spectroscopy only from localized areas such as Fe- and S-rich coatings and powdery particles attached on the surface of magnetic particles.

The XRD analysis revealed the presence of maghemite (γ-Fe_2O_3) in the Cogas magnetic fraction (Fig. 4b). The maghemite has 2.51-, 2.94-, and 2.03-Å diagnostic XRD peaks. The ferromagnetic maghemite would be formed as an alternative product of magnetite from ferrous iron minerals under an oxidation condition. The absence of diagnostic

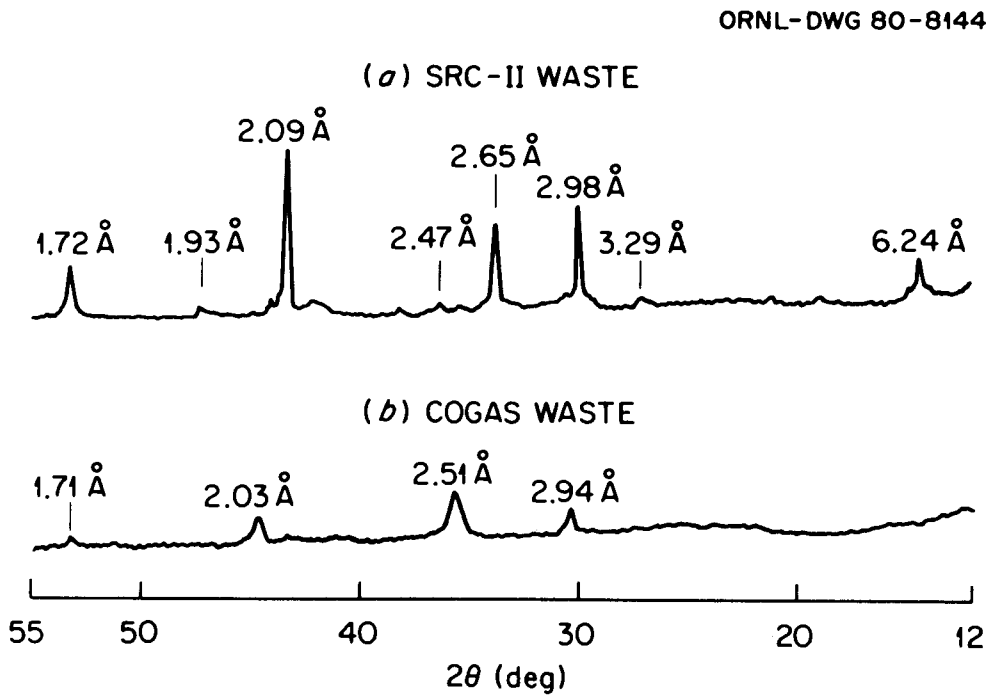

Fig. 4. X-ray diffractograms of ground ferromagnetic fractions from solid wastes. (a) Texaco (b) Cogas.

iron sulfide mineral peaks in the diffractogram indicated that the iron sulfide coatings and spherical inclusions were not crystalline minerals but ferromagnetic amorphous iron sulfides with mass deficits of sulfur in their structure.

Texaco waste could be characterized as ferruginous aluminosilicates. The Fe and S contents in the waste were much higher than in the other wastes (Table 2). The trace element concentrations in the waste were comparable to the Cogas waste. The composition of the Texaco magnetic fraction was dramatically different from the nonfractionated sample; the Fe and S contents were increased drastically in the magnetic fraction. Consequently, the elements commonly associated with silicate minerals and organic matter in coal were decreased in the magnetic fraction.

In the SEM micrograph of the magnetic fraction of the Texaco waste, the light-gray particles (marked m in Fig 3E) were dominated by Fe and S with a 1:1 x-ray spectral intensity ratio. The darker particles in the magnetic and nonmagnetic fractions (marked n in Fig. 3D and E) were dominated by Si and Al and to a lesser degree by Fe and S in the x-ray spectroscopic analysis. The nonmagnetic silicate particles in the magnetic fraction were carried by the magnetic particles in the aggregate. The light gray coatings on the surface of the nonmagnetic particles (arrow w in Fig. 3D) had Fe and S as major constituents. The intensity ratio of Fe to S on the iron sulfide coating varied, but the Fe intensity was always stronger than the S intensity in the x-ray spectra.

The XRD analysis revealed that pyrrhotite ($Fe_{1-x}S$) was the major component of the magnetic fraction showing 2.98, 2.65, and 2.09 Å peaks (Fig. 4a). Very weak diagnostic peaks (6.24, 3.29, and 1.93 Å), of lepidocrocite (γ-FeOOH) were also detected by XRD analysis. The rod-shaped iron mineral observed on the surface of the magnetic fraction (arrow s in Fig. 3C) could be the lepidocrocite mineral. The pyrrhotite was probably formed from pyrite (FeS_2) by gradual reduction of S under reducing conditions, while the lepidocrocite on the surface was formed from the pyrrhotite by oxidation and hydration processes ($2FeS + 4\text{-}1/2O_2 + 3H_2O \rightarrow 2FeOOH + 2H_2SO_4$) during storage of the waste.

Leaching Properties

The leaching characteristics of the solid wastes were determined using the proposed ASTM method and batch equilibrium method. The proposed ASTM method was intended as a rapid means of obtaining a leachate for determination of extractable components in wastes as well as for evaluation of the leachate in terms of environmental hazard of the waste. Therefore, some of the trace elements suspected to be potentially hazardous for the environment were selected for analysis in this study (Table 3). Most of the elements except Ni and Cu in the table were listed in the Interim Primary Drinking Water Regulations (IPDWR). With exception of Ni, the concentrations of the dissolved trace elements in both H_2O and NaOAc leachates were very low and were one tenth to one hundredth of those established in IPDWR.

Table 3. Batch-leaching results of British Gas-Lurgi, Cogas, and Texaco solid wastes obtained by proposed American Society for Testing and Materials methods

	British Gas-Lurgi		Cogas		Texaco	
Element and pH	H_2O	NaOAc	H_2O	NaOAc	H_2O	NaOAc
Concentration (ng/ml)						
Arsenic	1.50	5.3	< 0.5	< 0.5	< 5	< 5
Cadmium	0.058	0.27	7.0	5.2	4.0	4.9
Chromium	1.6	28	0.7	31	3.7	3.9
Copper	7.7	34	44	89	a	a
Lead	0.43	9.4	0.6	17	5.2	2.1
Mercury	0.023	0.043	0.013	0.014	0.025	0.010
Nickel	11.4	344	2500	2200	3032[b]	a
Selenium	< 5	< 5	< 0.05	< 0.05	0.04	0.04
Silver	0.14	0.14	< 0.05	0.32	0.04	0.23
pH[c]	7.2	4.5	4.6	4.5	4.7	4.5

[a]Not determined.

[b]Calculated from the data obtained by a batch experiment with solid-to-solution ratio of 1 to 16.

[c]pH of leachates.

In the H_2O leachates of the wastes, the dissolved Ni concentrations for the Cogas and Texaco wastes were considerably higher than for the British Gas-Lurgi waste. The H_2O leachate of the British Gas-Lurgi had lower Cd and Pb concentrations compared with the other wastes. There were no noticeable differences of concentrations of the other trace elements among the wastes. The pH of H_2O leachate of the British Gas-Lurgi was near neutral (7.2), and the others were mildly acidic (4.6). In the NaOAc leachate of the Texaco, the Cr and Pb concentrations were noticeably lower than in the other leachates, and the Cd concentration in the British Gas-Lurgi leachate was lower than the others. The buffer capacity of the NaOAc solution was able to maintain the pH (4.5) of the solution after mixing with different wastes.

The NaOAc leachates of the British Gas-Lurgi and Cogas wastes had higher concentrations of Cd, Cr, Cu, and Ni than the H_2O leachates of the wastes, but appreciable differences were observed between the NaOAc and H_2O leachates of the Texaco waste. For the British Gas-Lurgi, the considerable differences of leachate concentration could be attributed to the pH difference of the leachates. The differences of the Cogas leachates suggested that the acetate in the NaOAc solution might promote the leaching of the trace elements, but such evidence could not be confirmed from the Texaco results.

As an alternative approach, a batch equilibrium leaching experiment was conducted to test the long-term leachability of the wastes. The leaching data given in Table 4 were the average concentrations of duplicate batches. The concentrations of Ca, Al, Fe,

Table 4. Concentrations of selected elements in leachates of British Gas-Lurgi, Cogas, and Texaco solid wastes

Element	Concentration (μg/ml) after equilibrium time of -							
	0.2 day	1 day	5 days	10 days	20 days	30 days	60 days	113 days
				Cogas				
Ca	1.97	1.92	2.01	2.98	2.75	2.42	5.21	4.62
Al	0.15	0.17	0.18	0.29	0.36	0.27	0.63	0.89
Fe	0.19	0.47	0.37	0.50	0.59	0.54	0.55	0.10
Ni	0.28	0.38	0.51	0.58	0.56	0.64	0.88	1.01

Element	Concentration (μg/ml) after equilibrium time of -							
	5 days	10 days	20 days	30 days	40 days	50 days	60 days	165 days
				British Gas-Lurgi				
Ca	2.04	2.76	3.54	4.31	4.77	5.34	5.49	7.72
Al	0.36	0.68	0.92	1.09	1.11	0.98	1.06	1.20
Fe	0.76	0.42	0.03	0.02	0.02	0.23	0.01	0.20
				Texaco				
Ca	31.5	32.4	33.3	34.8	36.7	37.4	38.6	43.9
Al	0.11	0.12	0.12	0.26	0.40	0.58	0.80	0.63
Fe	74.5	80.0	81.5	82.5	92.0	96.0	98.0	102.0
Ni	0.84	0.64	0.50	0.49	0.39	0.35	0.35	0.18
S[a]	76	78	81	85	95	100	106	114

[a]Sulfate (SO_4) form of sulfur in leachate reported as S.

Ni, and SO_4 were determined instead of trace elements because most of the trace elements in the leachates were at concentrations near the analytical detection limit.

The experimental data (Table 4) were plotted as function of leaching concentration (C_w) versus time (t). Using the first order dissolution model, Eq. (3), "best" fitting estimates of the model parameters and their respective standard errors were obtained using the NLIN program (Table 5). The adequacy of the fitted model was evaluated by examining the magnitudes of the estimated standard errors relative to the estimated parameters as well as examination of plots of the residuals (difference between observed and estimated concentrations) vs time. Since the estimated standard error terms were relatively small in relationship to the parameters and no apparent patterns occurred in the residual plots (not shown), the model was felt to be adequate. That is, under the given experimental conditions, the conceptual model not only describes the intrinsic processes but could adequately predict concentration over time. Further testing of the adequacy of the model is needed, but it was limited in this study due to the small number of samples.

The readily dissolved components (C_i) in the leachates were contributed by the dissolution of weathered, precipitated, and adsorbed components on the waste, while the rate and time-related functional concentration (C_f) resulted from the dissolution of structurally bound components of the waste. Knowing the C_i and C_f concentrations at equilibrium and the rate constant (k), an expected leachate concentration could be predicted at a given wastewater contact

Table 5. Estimated dissolution constants from equilibrium batch leaching experiments of British Gas-Lurgi, Cogas, and Texaco solid wastes

Waste (equilibrium pH)	Element	Initially dissolved concentration, C_i (μg/ml)	Functional concentration at equilibrium, C_f (μg/ml)	Total concentration at equilibrium, C_w (μg/ml)	Rate constant, k ($days^{-1}$)	Distribution coefficient, D_d (ml/g)	Retardation coefficient, R_d
British Gas-Lurgi (pH 7.1)	Ca	1.69 (0.14)[b]	6.42	8.11	0.016 (0.001)[b]	22700	2270 (70)[b]
	Al	0 (0.25)	1.10	1.10	0.106 (0.030)	80000	8000 (290)
Cogas (pH 4.6)	Ca	1.86 (0.42)	3.52	5.38	0.018 (0.017)	5400	540 (150)
	Al	0.15 (0.01)	1.07	1.22	0.010 (0.003)	82700	8270 (1090)
	Fe	0.17 (0.03)	0.39	0.56	0.167 (0.037)	237500	23750 (850)
	Ni	0.37 (0.04)	0.71	1.08	0.020 (0.009)	240	24 (3)
Texaco (pH 4.5)	Ca	30.46 (0.29)	15.80	46.26	0.012 (0.001)	500	50 (1)
	Al	0 (0.18)	0.72	0.72	0.026 (0.017)	122100	12210 (3030)
	Fe	70.46 (3.34)	33.36	103.82	0.025 (0.007)	1700	170 (6)
	S	69.10 (3.50)	48.47	117.57	0.019 (0.005)	300	33 (1)

[a]Dissolution distribution coefficient (C_s/C_w) at equilibrium.

[b]Numbers in parentheses indicate asymptotic standard error.

time. The dissolution distribution constant (D_d) calculated from the retardation constant (R_d) is the ratio of a component in the waste to that in the leachate at equilibrium. Since the reciprocal of D_d is the fraction of the dissolved part against the remaining part in the waste, the D_d values could be used as a comparative measurement of the leachability of the components.

In the British Gas-Lurgi leachate, the Ni and SO_4 concentrations were too low to detect the changes during equilibration. The Fe concentration decreased as the equilibration progressed (Table 4), and the pH of the leachate did not change significantly. The readily dissolved Ca concentration (C_i) was 21% of the total dissolved concentration (C_w) at apparent equilibrium (Table 5). The Ca in the waste was dissolved with slower rate than Al, but the Ca was more leachable than the Al in the waste. The Al appeared to have reached equilibrium during the equilibration period.

The dissolved SO_4 concentration in the Cogas leachate was not monitored during equilibration, but it was 96 μg/ml at end of the period. About 40% of the total dissolved Ca concentration in the Cogas batches at equilibrium was leached within a short period of equilibration (Table 5). The D_d values indicated that Ca in the Cogas waste was more leachable than in the British Gas-Lurgi waste and less leachable than in the Texaco waste. The dissolved Fe concentration of the Cogas waste increased rapidly and then decreased after 60 d, suggesting that some of the dissolved Fe was either adsorbed or precipitated at the later stage of equilibration. The initially dissolved Ni concentration was 35% of the total concentration at

equilibrium. Although the rate constant of Ni was small, the D_d data revealed that the Ni was more leachable than the other elements in the waste. The dissolution pattern of the Al was very similar to the Ca and Ni (Fig. 5), although their concentrations were different in this weakly acidic (pH 4.6) leachate.

The dissolved Ca, Fe, Al, and S (as SO_4) concentrations in the Texaco batch increased slowly (Fig. 6). Although the total Ca concentration in the Texaco waste was lower than that for the other wastes, the total dissolved Ca concentration in the leachate was higher. The total dissolved Fe and SO_4 concentrations in the leachate were very high. The higher equilibrium concentrations of Fe (1.7 m$\underline{M}$) and S (3.5 m$\underline{M}$) with respect to the crystalline pyrrhotite solubility product ($K_{sp} = 10^{-15.2}$) suggest that the dissolving FeS components in the waste might be amorphous iron sulfide. The Ni concentration in the leachate decreased unexpectedly as the equilibration progressed. The gradual decrease of the initially dissolved Ni concentration in the leachate could be caused by the coprecipitation of Ni with ferric hydroxide formed in the solution and by the adsorption on residual carbon. The dissolution rate of the amorphous iron sulfide might be faster than the oxidation and precipitation reaction of the dissolved ferrous iron. The concentration of readily dissolved portions of Ca, Fe, and S, but not Al, was a major part of the total concentration at equilibrium. The dissolution distribution coefficient of Ca and Fe in Texaco waste was also very low as compared with the other wastes, suggesting that those elements in the Texaco waste are in a more leachable form as compared

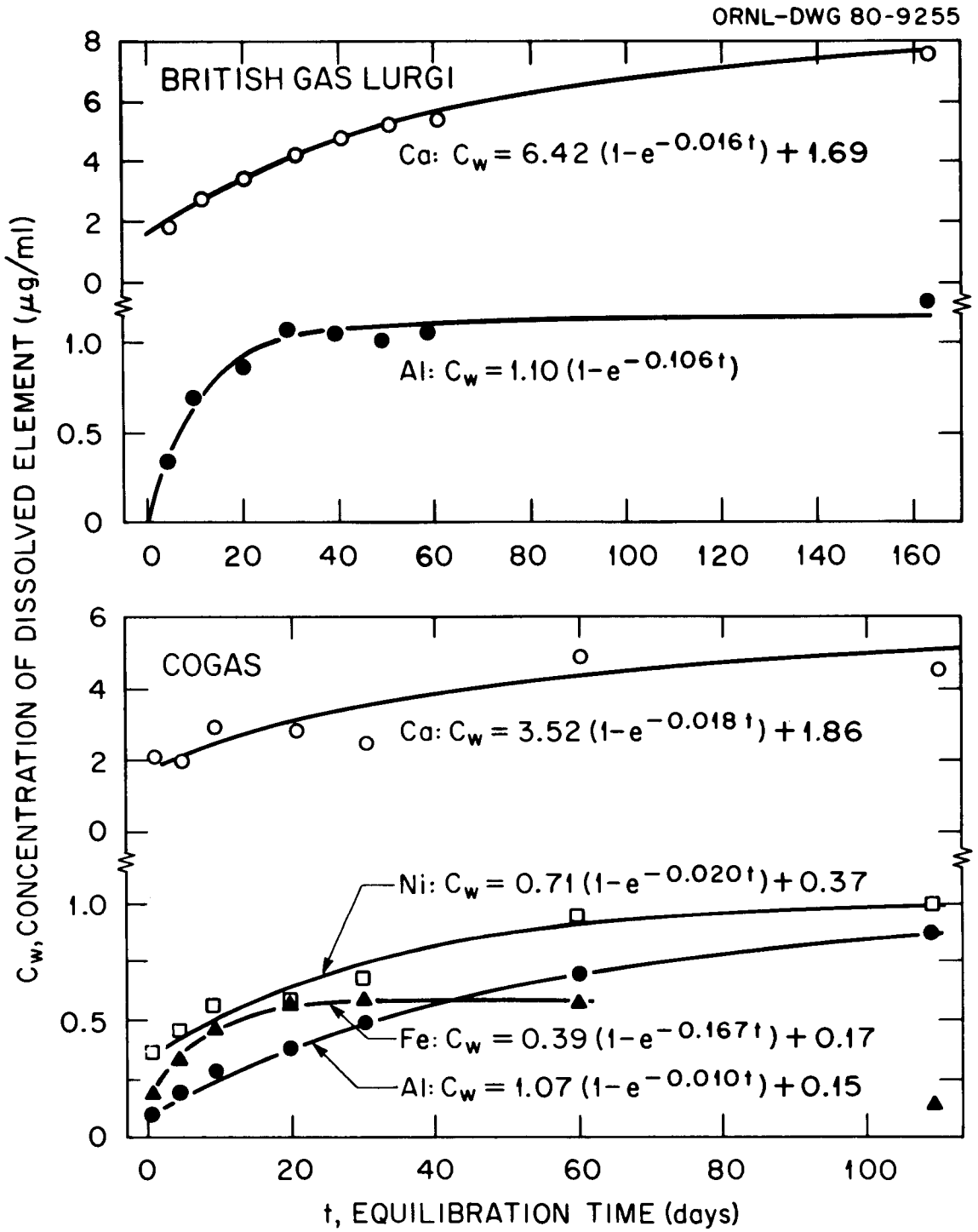

Fig. 5. "Best fit" dissolution curve and equations for the British Gas-Lurgi and Cogas wastes.

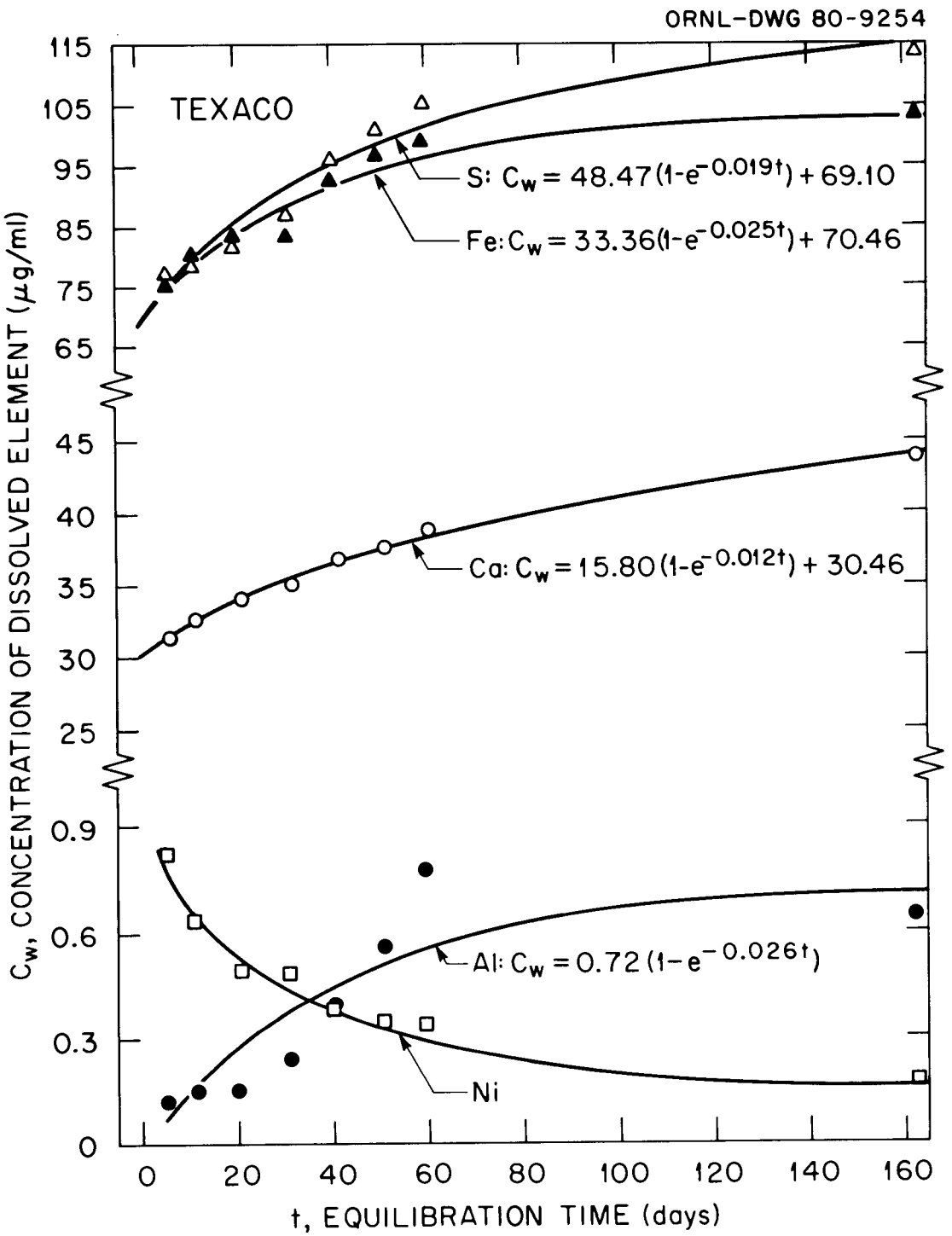

Fig. 6. "Best fit" dissolution curve and equations for the Texaco waste.

with the other wastes. The experimental results from the Texaco waste demonstrated the complexities involved in the leaching process. The surface properties, crystallinity, and chemical composition of the wastes are all important factors in the leaching process.

Although the equilibrium batch experiments did not monitor the concentration changes of the trace elements listed in the IPDWR, their leaching behavior could be predicted on the basis of similarity in chemistry with other elements studied, the short-term batch leaching results, and chemical composition of the wastes.

DISCUSSION

From the results of laboratory studies reported here it appears that the surface properties of the wastes, along with the elemental composition and distribution in the wastes, were the most significant factors controlling the leachability of the wastes. The physical properties of the wastes were determined by the specific operating conditions of each individual conversion process. Differences in the feed coal sources are expected to contribute very little to differences in the leachability of the wastes because the pilot plants used Appalachian or Eastern Interior coals which had similar chemical compositions with few exceptions (Zobovic, 1975).

The British Gas-Lurgi and Cogas wastes were composed of large vitreous particles and the surface of the particles was relatively clean in comparison with the extensively coated and relatively fine spherical Texaco waste. In the British Gas-Lurgi waste, the major and trace components were diluted by the limestone flux added during the

slagging process. As a result, the composition was significantly different from a conventional Lurgi process waste (Shriner et al., 1978) as well as from the Cogas and Texaco wastes (Table 2). The slagging process vitrified the coal ash, producing the calcic aluminosilicate glass. Other gasification processes such as Bigas and CO_2-acceptor also used limestone and produced Ca-rich wastes.

The Cogas and Texaco wastes were found to be composed of partially vitrified ferruginous aluminosilicates. The partial vitrification and morphological nonuniformity of the Cogas waste resulted from the temperature gradient which occurred in the reactor. The ferromagnetic fraction of the Cogas waste had immiscible iron sulfide (probably pyrrhotite) and iron oxide (maghemite) inclusions in the aluminosilicate matrix. In the Texaco waste, most of the silicate glass particles were coated with amorphous iron sulfide. The pyrrhotite particles in the waste might be formed during the liquefaction process, but the silicate slag was formed from mineral residue slurry during the gasification process. Mineralogical study of solid produced by the SRC-I process concluded that most of the pyrite in the feed coal was reduced to pyrrhotite during the liquefaction process (Wakeley et al., 1979).

Literature data (Straughan et al., 1978; Shriner et al., 1978; Filby and Khalil, 1978; Sather et al., 1975) for trace-element concentrations in coal fly ash, bottom ash, and conversion wastes are plotted along with the analytical results of the wastes studied here (Fig. 7). Although more data are needed for generalization, the limited data revealed that the concentration ranges of trace elements

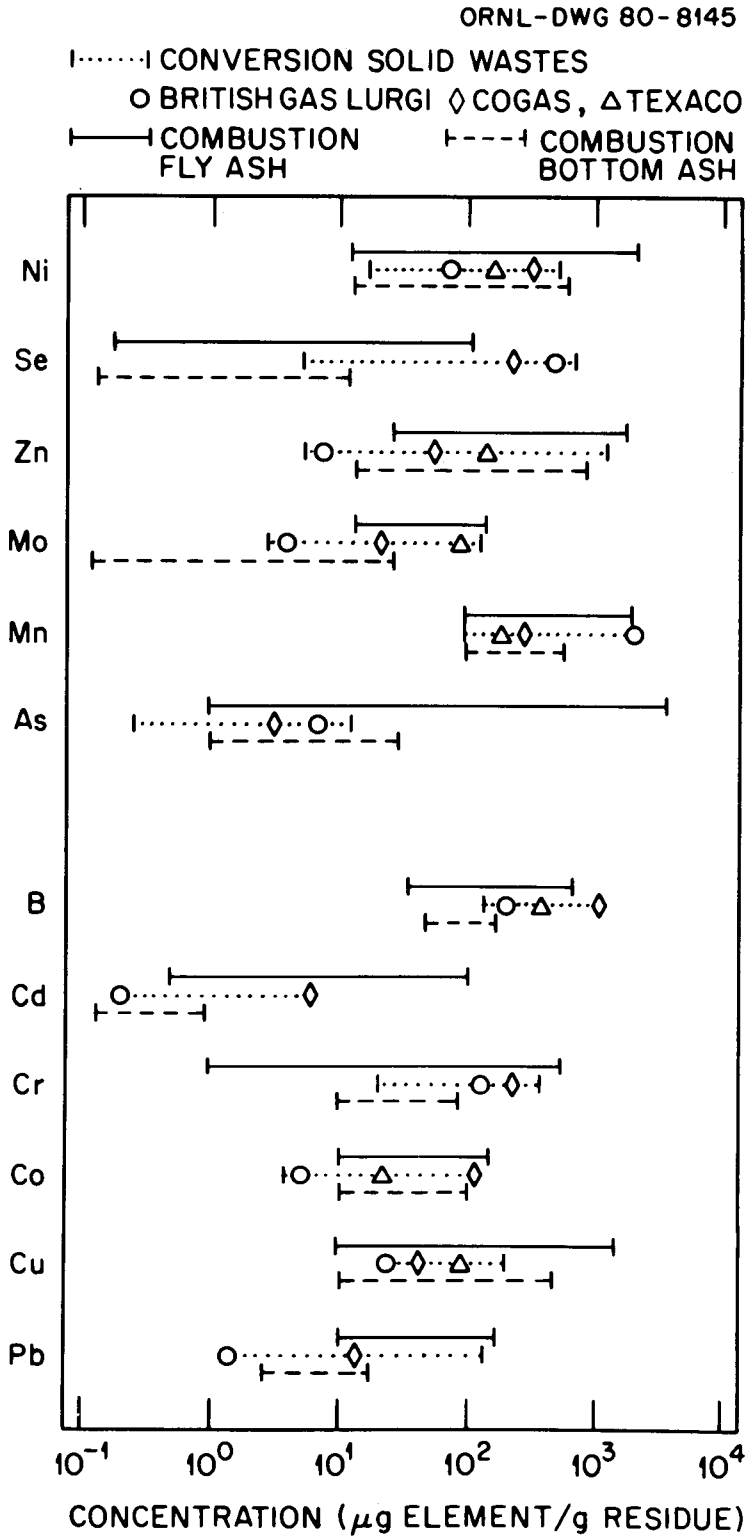

Fig. 7. Range of selected trace element concentrations in combustion solid wastes (fly and bottom ashes) and conversion solid wastes including the British Gas-Lurgi, Cogas, and Texaco.

in the conversion wastes lay between the concentration ranges of fly ash and bottom ash of combustion wastes except for selenium and boron. It has been known that fly ash has higher amounts of most trace elements than its counterpart of bottom ash and thus poses more environmental problems (Straughen et al., 1978).

The results of the ASTM batch leaching experiments revealed that the amount of trace elements released from each waste depended on the manner in which the elements were distributed and associated with the waste, along with the pH buffering capacity of the leaching solution. In the H_2O leachates, the concentrations of most trace elements, except Ni, were too low to evaluate the differences between the wastes. The relatively high Ni concentration in the Cogas and Texaco leachates appeared to be related to the higher Ni concentration in the Fe-rich coating on the surface of the wastes. Significant differences were found in the trace element concentrations between the H_2O and NaOAc leachates of the British Gas-Lurgi waste and minor differences for the Cogas. No significant differences were observed for the Texaco waste. The different responses of the wastes to the leaching solutions were caused largely by the pH differences among the wastes. The buffering capacity of the NaOAc solution held the pH of the British Gas-Lurgi leachate down to 4.5 but did not affect the pH values of the Cogas and Texaco leachate, which were close to 4.5 without the buffer solution.

The long-term equilibrium batch experiment was used to determine values for the first-order dissolution rate (k), equilibrium concentrations, and equilibrium dissolution distribution coefficients

(D_d). These are to be used to predict the concentration of potentially hazardous elements in ground water moving through a landfill. The readily dissolved components (C_i) comprise the major portion of the leaching solution in the early stages of the leaching process, but as soon as they were removed, the dissolution of elements from the wastes followed a first order kinetic reaction to a given functional concentration (C_f) at equilibrium with a dissolution rate k. The constants obtained from the long-term batch experiment can be used to a limited extent to estimate a leachate concentration of the initial and total concentration leached from the disposed waste at various hydrologic residence times. Such an estimation of the leachate concentration under a given disposal condition is the first step for any transport study of contaminants and for assessment of groundwater quality in the disposal area.

REFERENCES

Boegly, W. J., Jr. 1978. Solid waste management. pp. 23-31. IN Proc., Symposium of Potential Health and Environmental Effects of Synthetic Fossil Fuel Technologies. ORNL/CONF-780903. Oak Ridge National Laboratory, Oak Ridge, Tennessee.

Environmental Protection Agency (EPA). 1977. Simultaneous multielement analysis of liquid samples by inductively coupled organ plasma atomic emission spectroscopy. Region V, Central Regional Laboratory, Chicago, Illinois.

Feldman, C. 1979. Improvements in the arsine accumulation-helium glow detector procedure for determining traces of arsenic. Anal. Chem. 51:664-669.

Filby, R. H., and S. R. Khalil. 1978. Trace elements in the solvent refined coal processes, SRC-I and SRC-II. pp. 102-105. IN Proc., Symposium on Potential Health and Environmental Effects of Synthetic Fossil Fuel Technologies. ORNL/CONF-780903. Oak Ridge National Laboratory, Oak Ridge, Tennessee.

Ham, R. K., M. A. Anderson, R. Stegmann, and R. Stanforth. 1979. Comparison of three waste leaching tests. EPA-600 12-79-071. Environmental Protection Agency, Cincinnati, Ohio.

Hespe, E. E. 1971. Leach testing of immobilized radioactive waste solids. A proposal for a standard method. At. Energy Rev. 9(1):195-207.

Jones, H. T., H. M. Braunstein, and W. J. Boegly, Jr. 1978. Studies for design of a solid waste management program. pp. 246-256. IN Symposium of Environmental Aspects of Fossil Fuel Processing. Division of Fuel Chemistry, American Chemical Society.

Morris, S. C., P. D. Moskowitz, W. A. Sevian, S. Silberstein, and L. D. Hamilton. 1979. Coal conversion technologies: Some health and environmental effects. Science 206:654-662.

Oak Ridge National Laboratory (ORNL). 1979a. Environmental Analysis Procedure. Internal correspondence. Union Carbide Corporation, Nuclear Division.

Oak Ridge National Laboratory (ORNL). 1979b. Fossil energy program quarterly progress report for the period ending September 30, 1979. ORNL-5612. Oak Ridge National Laboratory, Oak Ridge, Tennessee.

SAS. 1979. SAS User's Guide. pp. 317-330. SAS Institute, Inc., Raleigh, North Carolina.

Sather, N. F., W. M. Swift, J. R. Jones, J. L. Beckner, H. J. Addington, and R. L. Wilburn. 1975. Potential trace element emissions from the gasification of Illinois coal. PB-241220. IIEQ75-08. NTIS.

Shriner, D. S., B. R. Parkhust, H. S. Arora, C. W. Gehrs, N. T. Edwards, and T. Tamura. 1978. Physical, chemical, and ecological characterization of solid wastes from a Lurgi gasification facility. pp. 181-192. IN Proc., Symposium on Potential Health and Environmental Effects of Synthetic Fossil Fuel Technologies. ORNL/CONF-780903. Oak Ridge National Laboratory, Oak Ridge, Tennessee.

INTERNAL DISTRIBUTION

1-2. S. I. Auerbach
3-7. W. J. Boegly, Jr.
8. C. R. Boston
9. M. G. Browman
10. D. K. Brown
11. K. E. Cowser
12. E. C. Davis
13. S. G. DeCicco
14. C. W. Francis
15. C. W. Gehrs
16. S. G. Hildebrand
17-21. S. Y. Lee
22. S. E. Lindberg
23. L. E. McNeese
24. R. M. Reed
25. L. W. Rickert
26. T. H. Row
27. T. Tamura
28. R. R. Turner
29. J. S. Watson
30. G. T. Yeh
31. Central Research Library
32-41. ESD Library
42-43. Laboratory Records Dept.
44. Laboratory Records, ORNL-RC
45. ORNL Y-12 Technical Library
46. ORNL Patent Office

EXTERNAL DISTRIBUTION

47. William J. Coppoc, Texaco, Inc., P.O. Box 509, Beacon, NY 12508
48. J. B. Dixon, Department of Soil and Crop Sciences, Texas A & M University, College Station, TX 77843
49. R. E. Franklin, Environmental Programs, DBER-DOE, Washington, DC 20545
50. C. Grua, Department of Energy, Washington, DC 20545
51. G. W. Heunisch, Conoco Inc., High Ridge Park, Stamford, CT 06904
52. G. J. Hyfantis, Jr., Tennessee Valley Authority, 401 Building, Chattanooga, TN 37401
53. M. L. Jackson, Department of Soil Science, University of Wisconsin, Madison, WI 53706
54. H. T. Jones, Department of Energy, Fossil Energy, Washington, DC 20545
55. T. K. Lau, Department of Energy, Fossil Energy, Washington, DC 20545
56. Robert A. Lewis, EV-34, GTN, Department of Energy, Washington, DC 20545
57. James Malcolm, Department of Energy, EF-308, ET-66, GTN, Washington, DC 20545
58. Helen McCammon, Director, Division of Ecological Research, Office of Health and Environmental Research, Department of Energy, Washington, DC 20545
59. W. E. Mott, Department of Energy, Assistant Secretary for Environment, Washington, DC 20545
60. Haydn H. Murray, Director, Department of Geology, Indiana University, Bloomington, IN 47405
61. William S. Osburn, Jr., Division of Ecological Research, Office of Health and Environmental Research, Department of Energy, Washington, DC 20545

62. F. L. Parker, Department of Civil and Environmental Engineering, Vanderbilt University, Station B, Nashville, TN 37235
63. R. Perhac, EPRI, P.O. Box 10412, Palo Alto, CA 94303
64. Douglas Pewlitt, Acting Director, Office of Energy Research, Department of Energy, Washington, DC 20545
65. Paul G. Risser, Department of Botany and Microbiology, University of Oklahoma, Norman, OK 73019
66. Allen M. Robin, Texaco, Inc., P.O. Box 400, Montebello, CA 90640
67. George R. Shepherd, Department of Energy, Room 4G-052, MS 4G-085, Forestal Bldg., Washington, DC 20545
68. Richard H. Waring, Department of Forest Science, Oregon State University, Corvallis, OR 97331
69. Robert L. Watters, Office of Health and Environmental Research, Department of Energy, Washington, DC 20545
70. V. E. Weaver, Department of Energy, Washington, DC 20545
71. F. J. Wobber, Department of Energy, Washington, DC 20545
72. Robert W. Wood, Office of Health and Environmental Research, Bldg. GTN, Germantown, MD 20767
73. A. F. Yen, International Coal Refining Company, P.O. Box 2752, Allentown, PA 18801
74. Office of Assistant Manager for Energy Research and Development, Department of Energy, Oak Ridge Operations, Oak Ridge, TN 37830

75-101. Technical Information Center, Oak Ridge, TN 37830

☆ U.S. GOVERNMENT PRINTING OFFICE: 1981-740-062/77